AIMS Materials Science, 10(3): 484–498.
DOI: 10.3934/matersci.2023027
Received: 10 February 2023
Revised: 10 May 2023
Accepted: 29 May 2023
Published: 20 June 2023

http://www.aimspress.com/journal/Materials

Research article

Experimental and computational investigations of structural and photoluminescence properties of PVK/SWCNTs nanocomposites

Boubaker Zaidi[1,2,*], Mohammed G. Althobaiti[3] and Nejmeddine Smida[4,5]

[1] Department of Physics, College of Science and Humanities, Shaqra University, Dawadmi 11911, Saudi Arabia
[2] Laboratoire de Synthèse Asymétrique et Ingénierie Moléculaire de Matériaux Organiques Pour L'électronique Organique LR 18ES19, Department of Physics, Faculty of Science, University of Monastir, Monastir 5019, Tunisia
[3] Department of Physics, Faculty of Science, Taif University, Taif 21974, Saudi Arabia
[4] Department of Chemistry, College of Science and Humanities, Shaqra University, Quwaiiyah 19257, Saudi Arabia
[5] Laboratory of Interfaces and Advanced Materials, Faculty of Science, University of Monastir, Monastir 5019, Tunisia

*** Correspondence:** Email: boubaker@su.edu.sa.

Abstract: A simple mechanical dispersion method was used to elaborate new nanocomposite from the combination of single walled carbon nanotubes (SWCNTs) and polyvinylcarbazole (PVK) polymer. The obtained samples were annealed at the moderate temperature of 333 K to achieve good dispersion and inhibit phase separation. Force constants calculations using Density Functional theory were correlated with FTIR measurements to support the interaction between both components. Raman scattering was used to check the dispersion state of SWCNTs on the PVK polymer. Optical absorption analysis and stationary photoluminescence and time resolved photoluminescence technics have been used to elucidate the change of optical properties after SWCNTs adding. The formation of bulk nano-hetero-junction resulting from the extended interfaces, leading to efficient dissociation of the charge pairs was shown by quenching effects in polymer photoluminescence when increasing SWCNTS contents. A noticeable decrease of the life time is observed by time resolved photoluminescence, which reflects the shortness of diffusion pathways and consequently an improvement of the electron transfer.

Keywords: SWCNTs; PVK; nanocomposites; Raman; photoluminescence; DFT

1. Introduction

Currently, organic photovoltaic (OPV) structures represent the most promising low cost devices considered as first concurrent to silicon solar cells technology. Indeed, the organic active materials offer the ease processing, flexibility and low cost of production [1,2]. Thus, a great deal of effort was devoted in the last two decades in both academic and industrial tasks in order to increase the power conversion efficiency and scale-up of the production processes [3]. In fact, this research field was motivated by the discovery of photo-induced electron transfer from the excited state of conjugated polymers to nanoparticles such as C_{60} or carbon nanotubes [4,5]. A noticeable power conversion efficiency from a prototype of photovoltaic devices based on polymer/nanoparticles interpenetrating networks were first demonstrated starting from 2008 [6]. Over three decades the functionalization process often resulted in higher charge separation and good collection efficiencies due to the formation of hetero-junctions at the nanometer scale where the power conversion efficiency has reached some values similar to that of the porous silicon [7]. In fact, the charge mobility in such carbon-based structures is better than in silicon ($\mu_n \approx \mu_p \approx 100–110\ cm^2 \cdot V^{-1}\ s^{-1}$) [8]. Moreover, carbon nanotubes as single- or multiwalled forms are characterized by a very high rigidity and excellent chemical stability, which offer good thermal properties to the resulting nanocomposite. Their distribution over the sample maximizes the interfaces, where photoexcitation can occurs and accelerates their diffusion and dissociation. It is obvious, that the good repartition will reduce the distance between the photogeneration and separation sites to be lower than the diffusion length [9,10]. Furthermore, once the charge transfer is established, CNTs can provide the efficient to the collecting electrodes. To achieve high performance, a higher weight concentration of nanoparticles ([6,6]-phenyl-C61-butyric acid methyl ester PCBM or SWCNTs) is required in order to create large number sites for exciton dissociation and an ideal percolation network for electron transport. However, the insolubility of carbon nanotubes in the organic solvents is the major handicap to limit a maximum concentration leading to better dispersion process [11].

Applications of carbon nanotubes in organic photovoltaic have been of much interest especially in the form of single wall carbon nanotubes (SWCNTs). The improvement was largely interpreted as the result of charge separation at polymer-SWCNTs interfaces and efficient electron transport through nanotubes [12]. Besides, for the device operation, due to their higher thermal conductivity, these nanotubes can be used also for outside thermal energy evacuation, which permits to avoid device malfunction and gives it longer lifetime [13]. It is to note that the exciton dissociation process can be further improved by uniform distribution of photo-generations sites over the bulk of organic matrix. If such configuration is achieved by arranging the donor and acceptor zones as interpenetrating network, we can exploit the whole active layer in the power conversion. Indeed, it is limited only to the junction in the case of conventional semiconducting micrometric P-N junction. It is important to note that solvent nature an important role in the quality of the resulting nanocomposite and therefore on its power conversion efficiency. We use therefore in this work two different halogenated solvents (chloroform and chlorobenzene) to prepare PVK/carbon nanotubes blends. In fact, we try to investigate the impact of solvent polarity on the SWCNTs dispersion process by using solvents with different polarity indices, especially knowing the high Vander walls

cohesive forces of these nanotubes. The obtained nanocomposites were studied by FTIR and Raman spectroscopies in order to confirm the formation of nano-junctions and to evaluate the nature of the dispersion states. Optical absorption analysis, Stationary and time resolved photoluminescence technics where used to investigate change of PVK optical properties after CNTs adding. Structural changes regarding the dispersion process influencing the charge separation process and excited states life time variation were evidenced.

2. Materials and methods

The PVK and SWCNTs structures have been fully optimized in their ground states without constraints using the B3LYP method (Becke three-parameter hybrid with non-local correlation of Lee–Yang–Parr) [14,15]. In fact, this approach is extensively applied to organic polymers and it is founded on DFT for uniform electron gas used with the 6-31G basis set [16,17]. For the PVK, which exhibits an oligomer structure, calculations were limited to four units as model structure. For SWCNTs, the model structure is a winding of two helices each graphene containing 14 units. It should be noted that the nanotube length is not considered in these calculations. Indeed, to reflect that you had to have a length of at least a hundred times larger than its radius; such a structure requires a very high number of atoms and therefore a huge memory preserved in the calculation.
The polyvinylcarbazole (PVK) and single walled carbon nanotubes (SWCNTs) are purchased from sigma–Aldrich. SWCNTs with diameter in the range of 1.2–1.5 nm and lengths between 2 and 5 μm were produced by electric arc technique [18,19]. Chloroform (Formula: $CHCl_3$ density at 300 K = 1.49 g/cm^3 and boiling temperature of 334 K) and chlobenzene (formula: C_6H_5Cl, density at 300 K = 1.11 g/cm^3 and boiling temperature of 405 K) were also purchased from sigma–Aldrich. The composite preparation is based on the mixing procedure of dispersed SWCNTs with the PVK polymer solution, as described in some reports [20]. The PVK is firstly dissolved in the solvent with the concentration of 5.0 mg/cm^3. Then, a solution of dispersed SWCNTs with the concentration of 0.3 mg/cm^3 is added with quantified volume in order to obtain the desired SWCNTs weight concentration. This mixing process has been accomplished instantaneously after the dispersion in order to exploit the SWCNTs dispersed state and ovoid the agglomeration process. The obtained mixture was then sonicated for 30 min. Silicon single crystals were used as substrates for FTIR analyses. For photoluminescence and Raman measurements, the prepared dispersions relative to diverse amounts were deposited by spin coating into glass substrates at room temperature. All substrates were successively cleaned with deionized water and ethanol using ultrasonically bath. The nanocomposite thin layers acquired after solvent evaporation were heated in an oven under dynamic secondary vacuum at 333 K for 1 h [21].

FTIR spectra were recorded on Bruker Vertex 70 interferometer with a resolution of 4 cm^{-1}. The Raman scattering analyses were carried out on a Fourier-Transform Raman spectrometer Bruker RFS 100, with a spectral resolution of 2 cm^{-1} and by using excitation laser wavelength of 1064 nm. Photoluminescence (PL) measurements were recorded on a Jobin-Yvon Flouorolog spectrometer. Time resolved PL spectra were recorded using regenerative amplified 78 femtosecond laser system, which delivers 100 pulses at 1 kHz, 800 nm and 1 W. The optical absorption spectra are recorded using UV1800 spectrophotometer working in the absorption mode with the wavelength varying from 200 nm (6.2 eV) to 2,000 nm (0.62 eV).The samples were excited at 400 nm and the time-

resolved emission spectra were spatio-temporally detected using a high dynamic range Hamamatsu C7700 streak camera with temporal resolution <20 ps.

3. Results and discussion

In order to examine the eventual reactive sites in the carbon nanotubes and PVK backbone, the force constants between the nearest neighboring carbon atoms have been calculated in both the neutral and the oxidized states for the polymer and CNT optimized structures (Figure 1). The most apparent change is related to the force constants F_9, F_{10} and F_{11} in the case of PVK macromolecules (Table 1). These forces act between adjacent aliphatic carbon atoms in the –CH–CH_2– units. However, in the case of CNTs, the most significant changes are limited to the constant F_1, F_2 and F_3, resulting from neighboring carbon atoms located on the tube sides. These changes are indicators of the most probable reactive sites.

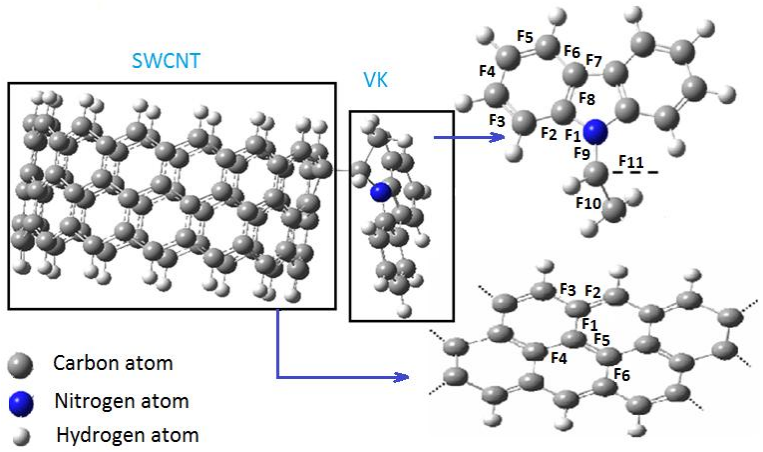

Figure 1. Force constants between neighboring atoms for PVK and CNT moieties in the PVK/CNT composite.

Table 1. Force constants expressed in millydyne/Å for PVK and SWCNTs at their neutral and oxidized states.

		F_1	F_2	F_3	F_4	F_5	F_6	F_7	F_8	F_9	F_{10}	F_{11}
PVK	Neutral state	6.38	6.28	6.48	6.06	6.49	6.27	5.37	5.70	5.66	7.72	4.72
	Oxidized state	5.57	6.44	6.40	6.16	6.40	6.42	5.24	5.89	7.14	6.58	7.38
SWCNTs	Neutral state	5.28	5.60	5.34	5.50	5.59	5.28	-	-	-	-	-
	Oxidized state	4.87	5.00	5.54	5.53	5.52	5.46	-	-	-	-	-

Therefore, if the functionalization between PVK and SWCNTs is governed by a grafting process, the covalent bonding will be probably between C-C aliphatic sequences of PVK and carbon constituting the tube end. This grafting process (Figure 2) can be tracked by FTIR analysis [22]. To support the eventual grafting process between PVK and CNT moieties, the nanocomposites elaborated either in chloroform or in chlorobenzene solvent were investigated using FTIR

spectroscopy. In the case of the composite prepared in chloroform, the appearance of a novel band at 1297 cm^{-1} in the FT-IR spectrum (Figure 3b–d) reveals the creation of a new C–C vibration that traduces the covalent bonding between CNTs and PVK. Besides, several bands of relatively high intensities, located at 418, 840, 1324, 1402, 1481, 1596, and 1624 cm^{-1} disappear in the composite spectrum in comparison with the PVK spectrum. These bands mainly reflect the different vibrational modes of the aliphatic –CH–CH_2– groups in the polymer. Moreover, the bands allied to the CH deformation and rocking, which appear at 717 and 742 cm^{-1}, were severely reduced. This results permit to evidence that the grafting process between CNTs and PVK is done locally through these groups, as suggested by force constants calculation.

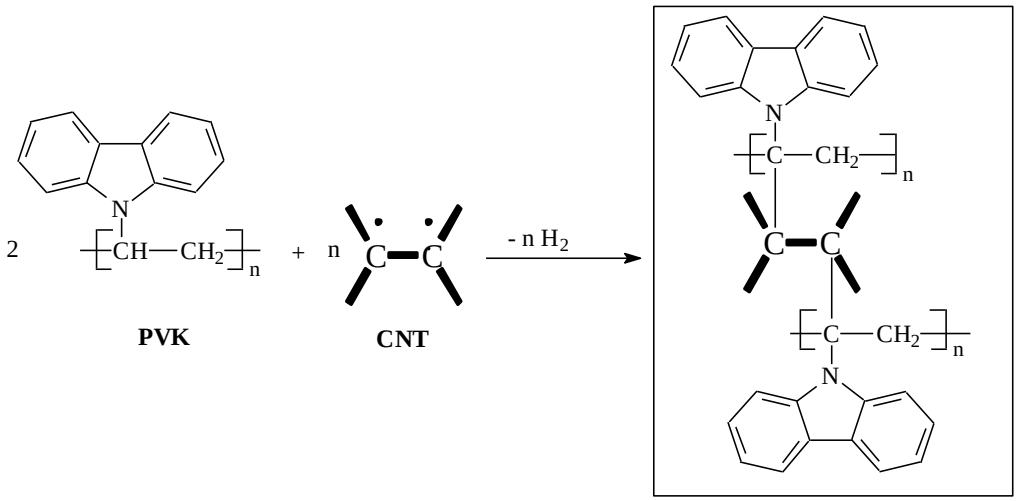

Fugure 2. The grafting mechanism between PVK and CNTs.

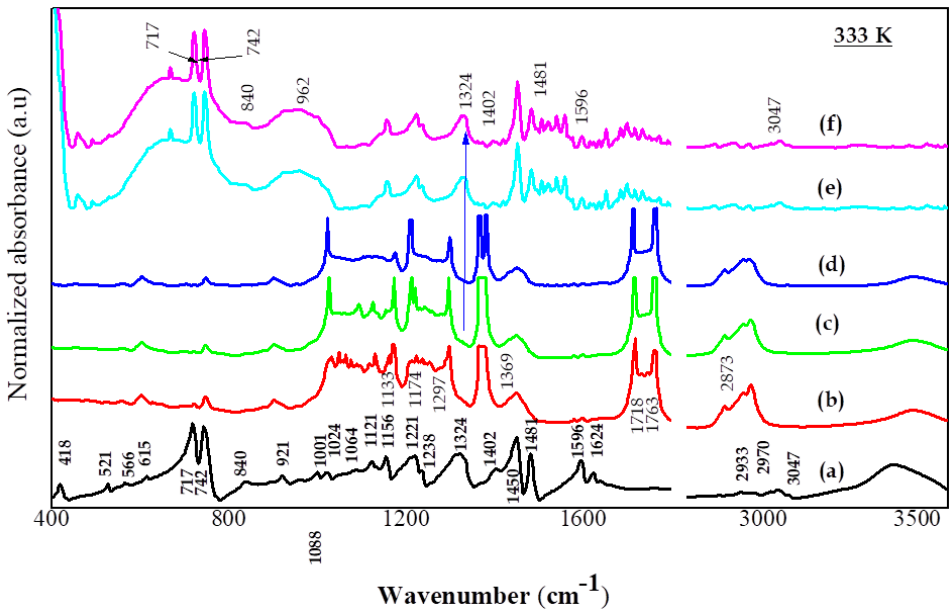

Figure 3. FTIR spectra of native PVK (a) and of PVK/CNT composites prepared using chloroform (1.5%) (b) and using chlorobenzene at CNT weight fractions of 0.85% (c), 1.10% (d), 1.75% (e) and 3.50% (f) (all annealed at 333 K).

In the case of composite prepared in chlorobenzene, the nanocomposite was elaborated at different concentrations which were able to reach 3.5% in nanotubes. This indicates that this polar solvent is adequate to obtain a good SWCNTs dispersion process. At low concentrations (0.85 and 1.10%), the recoded spectrum is similar to that obtained when using chloroform as solvent. The shape of the FTIR spectra was significantly modified in comparison with native PVK and new bands appear (Figure 3c,d). The bands located at 1174, 1718 and 1763 cm^{-1} are the signatures of C–C vibration relative to CNTs [23]. Other modes which appear approximately at 1133, and at 1297 cm^{-1} are respectively assigned to the in plane deformation of CH_2 group and the stretching of new C–C bond between the PVK and CNTs. Furthermore, the vibrational modes at frequencies of 418, 840, 1324, 1402, 1481, 1596 and 1624 cm^{-1} completely disappear, similarly to the case of chloroform solvent. These bands are mainly assigned to –CH–CH_2– units. It is believed that while the same grafting process has established in the case of chloroform solvent, the chlorobenzene permits this bonding only at low concentrations.

The CNTs dispersion on the organic material and the quality of the resulting composite were checked by changes in the radial and tangential modes of CNTs observed in the Raman spectra [24]. The Figure 4 represents differences between the elaborated nanocomposites, which can be a direct support to evidence the solvent nature effect on the dispersion of nanoparticles in polymer matrix. Compared to the spectrum of native SWCNTs, we notice a slight shift to lower wavenumbers for both radial and tangential modes due to the charge transfer from PVK to the CNT [25]. When using the chlorobenzene solvent, the mode at 181 cm^{-1}, assigned to the bundled form of CNTs, is severely reduced. CNTs exhibit therefore uniform distribution in the PVK matrix with mean diameter of d = 1.35 nm, as evaluated from the empiric relation $\upsilon = 223.75/d$ at 166 cm^{-1} [26]. The decrease in the relative intensity of peak at 1571 cm^{-1} illustrates structural change from two- to three-dimensional form in CNT network [27].

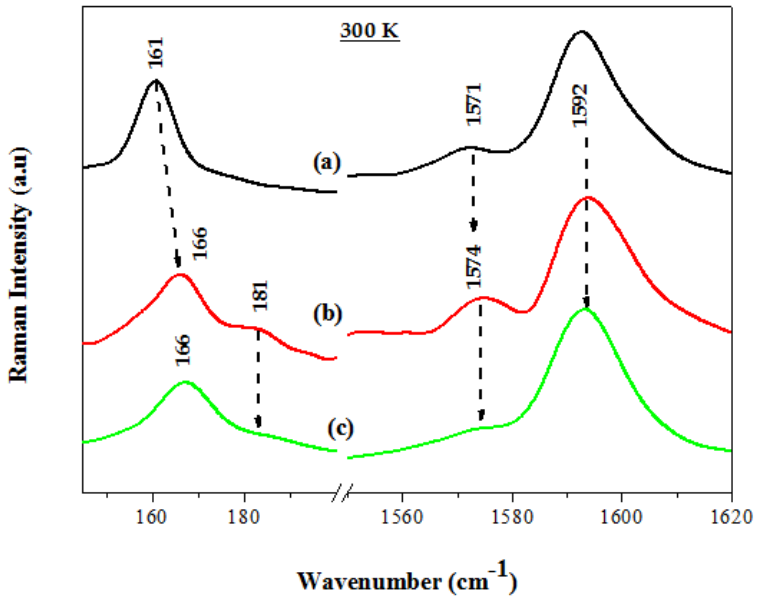

Figure 4. Radial and tangential modes changes for SWCNTs (a), PVK/SWCNTs (1%) elaborated in chloroform (b) and in chlorobenzene (c) (annealed at 300 K).

However, for the higher CNT concentrations (3.5%) (Figure 5), the quantity of polymer chains inserted between the individual tubes seems insufficient to allow the isolation of SWCNTs bundled forms. For this concentration, the intensive SWCNTs cohesive forces overcome the potential introduced by dispersion process.

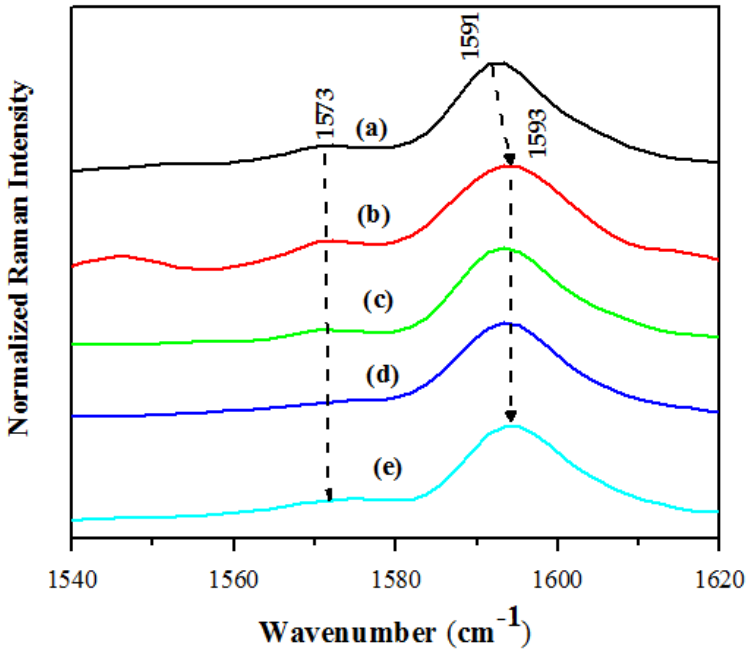

Figure 5. Tangential modes changes for SWCNTs (a) and the PVK/SWCNTs composites obtained in chlorobenzene at CNT weight fractions of 0.85% (b), 1.10% (c), 1.75% (d) and 3.50% (e) (annealed at 333 K).

The electronic interactions in excited state between PVK and nanotubes in the composite structures were investigated by photoluminescence spectroscopy. In comparison with native PVK, a slight redshift and a significant reduction in the emission intensity were observed for the nanocomposites elaborated in the chloroform (Figure 6b). In fact, the quenching effect suggests an energy transfer process from the photoluminescent polymer to the carbon nanotubes [28,29]. Otherwise, numerous recent studies showed the important improvement of the light harvesting efficiency and the photovoltaic performance of the organic photoactive layers owing to the energy transfer process [30], what makes such photoluminescent polymer/SWCNTs composites good candidates for solar cell applications. For the nanocomposites prepared in chlorobenzene with CNT weight concentration less than 1.75%, an exponential evolution of quenching effect with CNT ratio was observed, which is attributed to formation of complex in the ground state and exciplex in the excited state. For a CNT concentration of 1.75% the significant quenching of luminescence makes it possible to suggest a more accentuated energy transfer [31]. Indeed, referring to the intensity delivered by the native PVK, we can deduce that a high fraction exceeding 60% of the photo-excited carriers recombine through non-radiative processes. In fact, if excitons are efficiently dissociated, the direct excitons recombination will be limited and the photoluminescence will be quenched. This is why carbon nanotubes are known to be efficiently exploited as electron acceptor in organic solar cells [32,33].

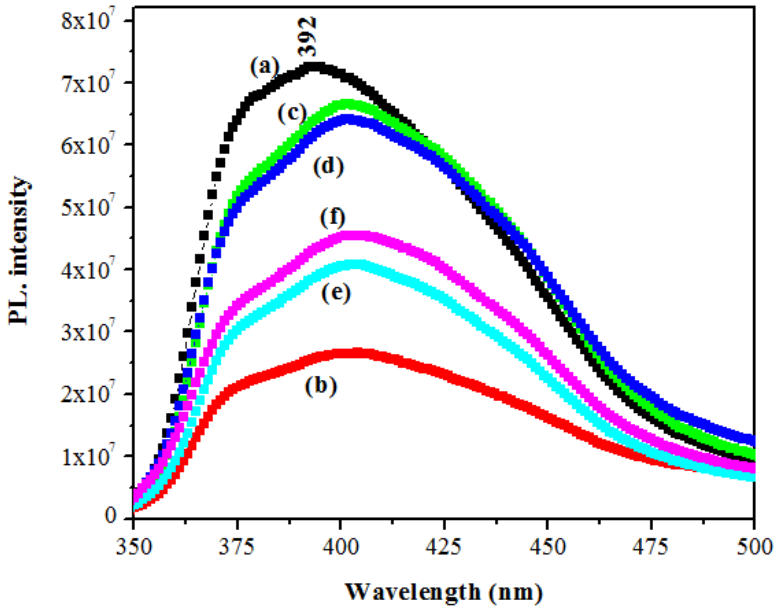

Figure 6. Photoluminescence spectra of PVK (a) and PVK/SWCNTs composites elaborated in chloroform (1.5%) (b), and in chlorobenzene at CNT weight fractions of 0.85% (c), 1.10% (d), 1.75% (e) and 3.50% (f) (excitation wavelength: 280 nm).

The optical absorption spectra for optimal concentrations in the case of chloroform or chlorobenzene are depicted in Figure 7. Both spectra are compared to that of original material (PVK). As previously reported in the literature, the main absorption bands of PVK are shown at 232, 260, 294, 330 and 343 nm [34]. After adding SWCNTs and for wavelengths longer than 360 nm, PVK is transparent. Then, by referring to the PVK spectrum, the two bands at 232 and 343 nm sudden a slight red shift to 237 and 352 nm respectively. This red shift can be attributed to the interaction between SWNTs and PVK as it is reported in the case of multi-walled carbon nanotubes (MWCNs) [35]. For wave length higher than 360 nm, the spectrum shows a large absorption band in the visible and near infrared regions, similarly as the case of the same composite prepared PVK functionalized carbon nanotubes [36]. Similar effect has been also demonstrated in the case of SWNTs/polyaniline obtained by an electro-synthesis process [37]. It is to note that SWCNTs alone present three bands in this spectral region peaked at 720, 976 and 1823 from which the last band (1823 nm) is the most intense and is attributed to the inter-band optical transition in the semi conducting SWNTs. Therefore, adding SWCNTs leads to broader absorption band giving a good compatibility with the solar spectrum. Such behavior proves also that PVK is good functionalized at lower SWCNTs concentrations.

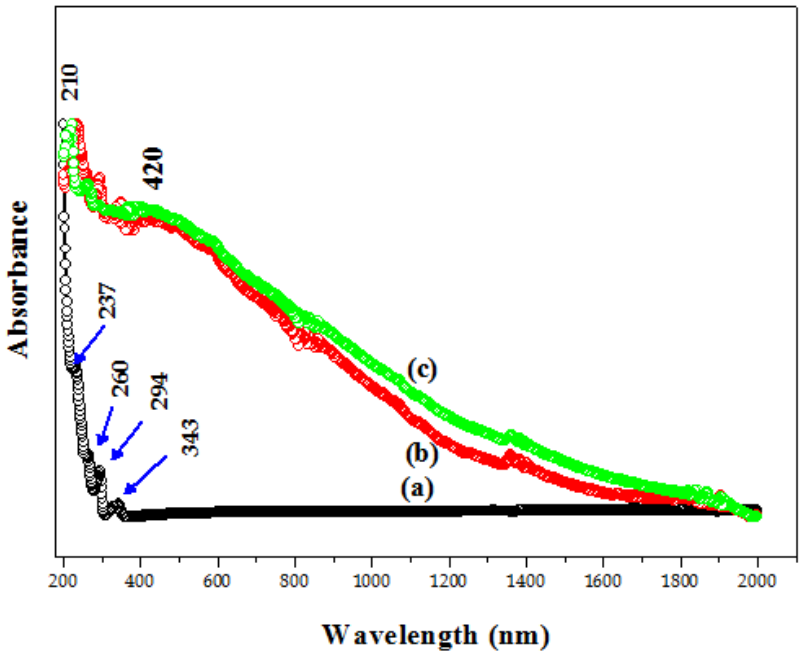

Figure 7. Optical absorption spectra of PVK thin film (a), PVK/SWNTs nanocomposites obtained using chloroform at 1.5% (b) and using chlorobenzene at 1.75 w% (c).

The PL cartography of the elaborated nanocomposites demonstrates that there are two contributions to luminescence process either the composite were prepared in chloroform or in chlorobenzene (Figure 8). It is therefore assumed that the normalized PL intensity decay times are very well simulated with two coupled exponential decays and by taking into account the contribution of apparatus function given by the Gaussian temporal dependence G(t) (Eq 1) of the laser pulse [38]. Likewise, we assumed that photobleaching or biexciton collisions can be neglected in our experiments.

$$G(t) = \frac{1}{\sigma\sqrt{2\pi}} \exp\left(-\frac{(t - t_0)}{2\sigma^2}\right) \tag{1}$$

The total population of excited species is expressed as $N = A_1N_1 + A_2N_2$, N_1 and N_2 represent the total populations of photogenerated charges in the energy states 1 and 2 (Eqs 1–3). A_1 and A_2 are proportional to the PL intensity from levels 1 and 2, respectively. τ_1 and τ_2 are their decay times, where $\beta_1 = 1/\tau_1$ and $\beta_2 = 1/\tau_2$.

$$\frac{dN_1(t)}{dt} = G(t) - \beta_1 N_1(t) \tag{2}$$

$$\frac{dN_2(t)}{dt} = \beta_1 N_1(t) - \beta_2 N_2(t) \tag{3}$$

In this simple model [39], the populations of levels 1 and 2 are coupled in order to account indirectly for a migration process from the short to the long segments. Photogenerated charges populating the higher energy level 1 migrate toward defects and fast relax on the lower energy state 2

with lifetime τ_1. At a longer time, the photogenerated charges on level 2 are less mobile and consequently survive longer with a slower time constant τ_2.

In order to show the average trend of the photogenererated charge migration time, we define below (Eq 4) an average decay time called $\tau_{average}$.

$$\tau_{average} = \frac{\sum_i A_i \tau_i^2}{\sum_i A_i \tau_i} \quad (4)$$

The PL decay of curves of the nanocomposites and of the PVK-SWCNTs solutions were depicted in Figure 9. Whereas, the inserting of SWCNTs in the polymer matrix results in quenching effects either for chloroform or chlorobenzene solvents, there are some differences on the dynamic parameters of the excited states (Table 2). In both cases, whatever the state is there are two populations with a specific life time and weight and an appropriate decay time. For the native polymer, in the case of chloroform there are two contributions (with faster and longer decay times) with approximately the same weights P_1 and P_2 which were evaluated according to the Eq 5.

$$P_i(\%) = \frac{A_i \tau_i}{\sum_i A_i \tau_i} \quad (5)$$

The use of chlorobenzene induces a more slowly contributions reaching the decay time 1.464 and 7.874 ns respectively for the first and the second contribution, while the values were of 1.335 and 5.181 ms in the case of chloroform. This can be attributed to the effect of solvent polarity on the chain spatial arrangement. This can be attributed to the more adequate alignment of the polymer chains in chlorobenzene, which suggest longer diffusion pathways leading to higher decay times [40].

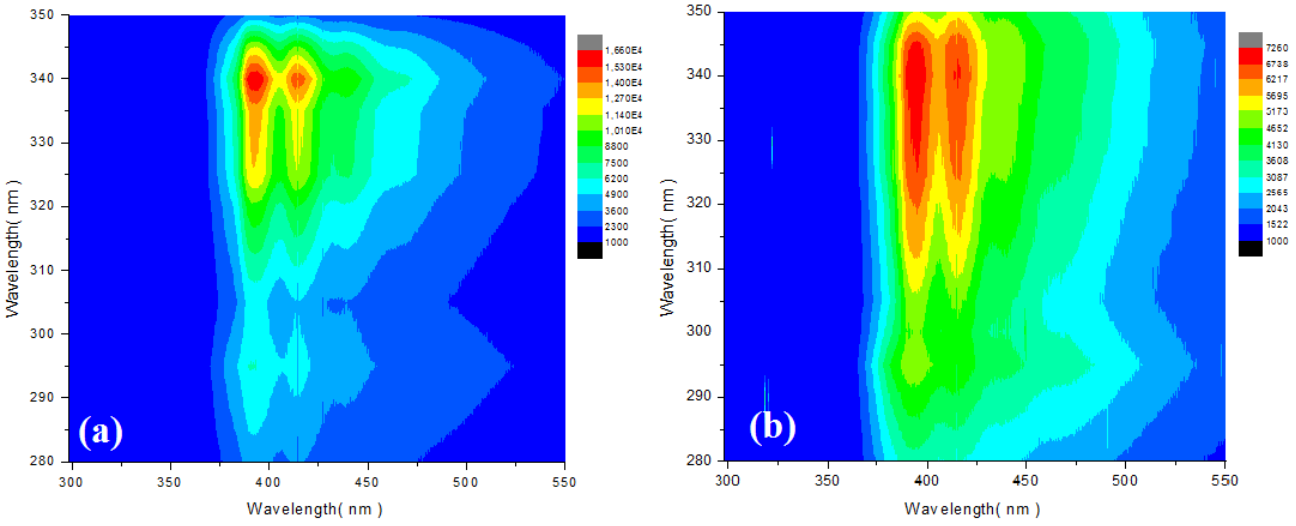

Figure 8. PL cartography of PVK/SWCNTs prepared in chloroform (a) and prepared in chlorobenzene (b).

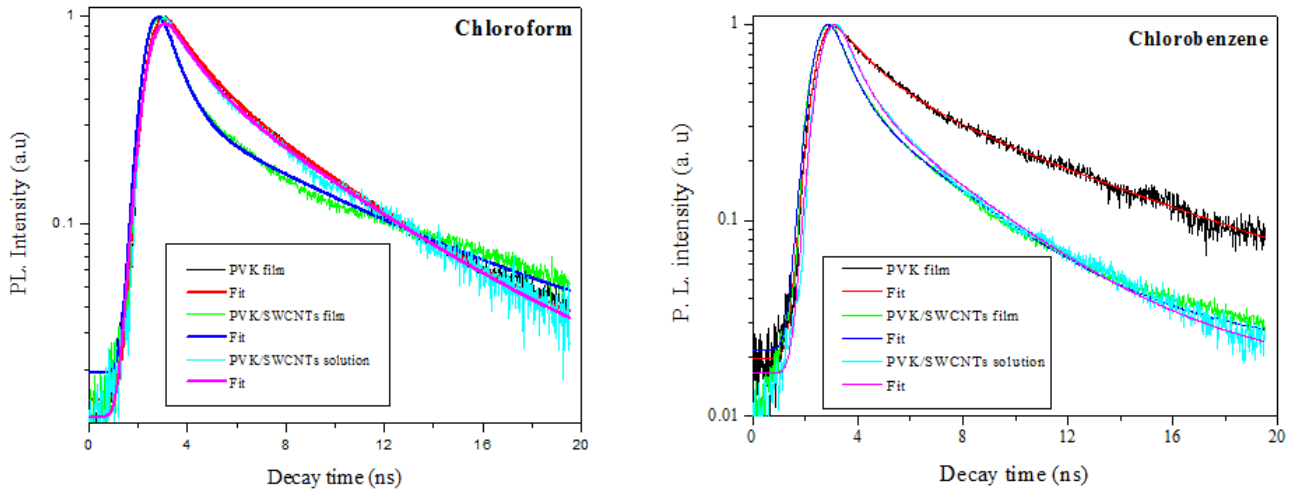

Figure 9. PL decay curves of the PVK film, nanocomposites films and PVK-SWCNTs solutions. (CNT weight fractions: 1.5% in chloroform; 1.75% in chlorobenzene).

Table 2. PL decay characteristics of native PVK, PVK/SWCNTs composite films and PVK-SWCNTs solutions.

		A_1	A_2	τ_1 (ns)	τ_2 (ns)	τ_a (ns)	P_1	P_2
Chloroform	PVK film	0.768	0.641	1.335	5.181	4.270	0.23	0.76
	Nanocomposite film	1.603	0.357	0.730	6.896	4.900	0.32	0.67
	PVK-SWCNTs solution	0.793	0.610	1.206	5.263	4.330	0.22	0.77
Chlorobenzene	PVK film	0.970	0.656	1.464	7.874	6.490	0.21	0.78
	Nanocomposite film	1.840	0.644	0.660	3.846	2.797	0.32	0.67
	PVK-SWCNTs solution	1.404	0.524	0.740	4.016	2.930	0.33	0.66

After adding carbon nanotubes to the PVK matrix in solid state, the weight of the first population (with shorter decay time) is increased and those of the second population is decreased (Table 2). This can be interpreted as the shortness of the radiative pathways correspondent to τ_2 after inserting SWCNTs. For the obtained nanocomposites, it is clearly seen that the used solvent has an important role in the life times and the radiative pathway length. In fact, in comparison with chloroform, the chlorobenzene leads to shorter average life time. This behavior can be explained by a better SWCNTs dispersion in the case of chlorobenzene solvent. This hypothesis is coherent by the decrease of the RBM mode at 181 cm^{-1}, assigned to the bundled form SWCNTs (Figure 4). These results are in full accordance with the progressive decrease in emitted energy intensity as a function of time from 0 to 1 ns obtained in 3D maps (Figure 10).

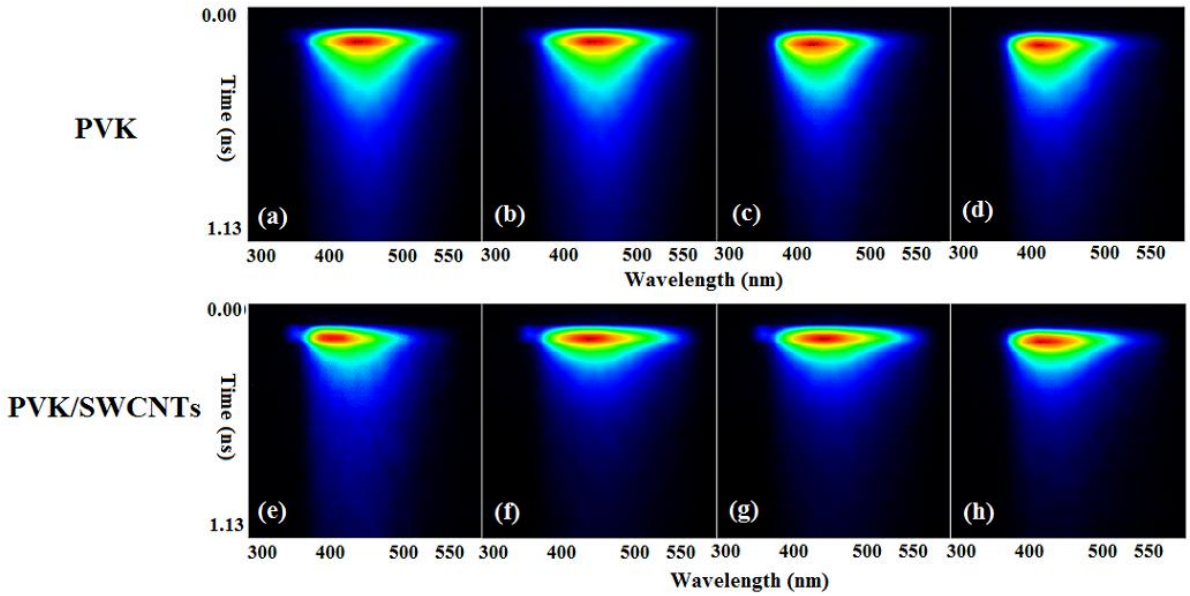

Figure 10. Contour plot of transient PL for PVK thin film prepared from chloroform (a), PVK thin film prepared from chlorobenzene (b), PVK in chloroform solution (c), PVK in chlorobenzene solution (d), PVK/SWCNTs composites prepared from chloroform (e), PVK/SWCNTs composites prepared from chlorobenzene (f), PVK-SWCNTs chloroform solution (g) and PVK-SWCNTs chlorobenzene solution.

4. Conclusions

Force constant variation from neutral to oxidized states and FTIR spectra of PVK/SWCNTs composites at different carbon nanotubes concentrations demonstrate that there is a grafting process between both components. The linkage is established at low CNT concentrations between the PVK–CH–CH_2– groups and the side wall of SWCNTs. The charge transfer is supported by PL quenching in both investigated solvents and it is more efficient in the case of chloroform. Moreover, the Raman spectroscopy demonstrated that the chlorobenzene leads to a more dispersed states for the SWCNTs. The photoluminescence cartography evidenced two exciton populations which contribute to emission of the nanocomposites. Therefore, the time resolved photoluminescence spectra are simulated with two coupled exponential decays. The results showed that dynamic parameters of the excited states are influenced by the solvent nature. Indeed, the use of chlorobenzene induces a quicker decay in comparison to chloroform. This effect has been interpreted as the consequence of the quality CNTs dispersion in the organic solvent. This hypothesis is supported by decrease in emitted energy intensity as a function of time. Regarding the dispersion states and the decay time variation, the obtained results let to conclude that the nanocomposite obtained using chlorobenzene with 1.75% CNT weight fraction is more efficient in photovoltaic applications.

Use of AI tools declaration

The authors declare they have not used Artificial Intelligence (AI) tools in the creation of this article.

Acknowledgments

The authors extend their appreciation to the Deputyship for Research & Innovation, Ministry of Education, Saudi Arabia, for funding this research work through project number IFP-2021-109.

Conflicts of interest

The authors declare no conflict of interest.

References

1. Rahlves M, Rezem M, Boroz K, et al. (2015) Flexible, fast, and low-cost production process for polymer based diffractive optics. *Opt Express* 23: 3614. https://doi.org/10.1364/OE.23.003614
2. Mahmoudi C, Muzuzu W, Fall S, et al. (2022) Near ultra-violet absorbers for transparent organic solar cells. *Dyes Pigments* 207: 110752. https://doi.org/10.1016/j.dyepig.2022.110752
3. Alkhalayfeh MA, Aziz AA, Pakhuruddin MZ (2021) Enhancing the efficiency of polymer solar cells by embedding Au@Ag NPs Durian shape in buffer layer. *Sol Energy* 214: 565–574. https://doi.org/10.1016/j.solener.2020.12.010
4. Zaidi B, Smida N, Althobaiti MG, et al. (2022) Polymer/carbon nanotube based nanocomposites for photovoltaic application: Functionalization, structural, and optical properties. *Polymers* 14: 1093. https://doi.org/10.3390/polym14061093
5. Muchuweni E, Mombeshora ET, Martincigh BS, et al. (2022) Recent applications of carbon nanotubes in organic solar cells. *Front Chem* 9: 733552. https://doi.org/10.3389/fchem.2021.733552
6. Yun D, Feng W, Wu H, et al. (2008) Controllable functionalization of single-wall carbon nanotubes by in situ polymerization method for organic photovoltaic devices. *Synthetic Met* 158: 977–983. https://doi.org/10.1016/j.synthmet.2008.06.025
7. Jia T, Zhang J, Zhong W, et al. (2020) 14.4% efficiency all-polymer solar cell with broad absorption and low energy loss enabled by a novel polymer acceptor. *Nano Energy* 72: 104718. https://doi.org/10.1016/j.nanoen.2020.104718
8. Zhu H, Wei J, Wang K, et al. (2009) Applications of carbon materials in photovoltaic solar cells. *Sol Energ Mat Sol C* 93: 1461–1470. https://doi.org/10.1016/j.solmat.2009.04.006
9. Saaidia A, Saidani MA, Romdhane S, et al. (2017) Morphology-dependent exciton diffusion length in PPE-PPVs thin films as revealed by a Forster mechanism based-study. *Synthetic Met* 226: 177–182. https://doi.org/10.1016/j.synthmet.2017.02.023
10. Saoudi M, Ajjel R, Zaidi B (2016) Experimental and theoretical study on the charge transfer between polyaniline and single walled carbon nanotubes. *J Mater Environ Sci* 7: 4435–4447.
11. D éz-Pascual AM (2021) Chemical functionalization of carbon nanotubes with polymers: A brief overview. *Macromol* 1: 64–83. https://doi.org/10.3390/macromol1020006
12. Sun Y, Zhang W, Chi H, et al. (2015) Recent development of graphene materials applied in polymer solar cell. *Renew Sust Energ Rev* 43: 973–980. https://doi.org/10.1016/j.rser.2014.11.040

13. Zhan H, Chen YW, Shi QQ, et al. (2022) Highly aligned and densified carbon nanotube films with superior thermal conductivity and mechanical strength. *Carbon* 186: 205–214. https://doi.org/10.1016/j.carbon.2021.09.069
14. Becke AD (1993) Density-functional thermochemistry. III. The role of exact exchange. *J Chem Phys* 98: 5648–5652. https://doi.org/10.1063/1.464913
15. Lee C, Yang W, Parr RG (1988) Development of the Colle-Salvetti correlation-energy formula into a functional of the electron density. *Phys Rev B* 37: 785–789. https://doi.org/10.1103/PhysRevB.37.785
16. Chouk R, Bergaoui M, Jaballah N, et al. (2019) Shedding light on structural, optoelectronic and charge transport properties of PPV stereoisomers for multilayer OLED application: A first principle computational studies. *J Mol Liq* 284: 193–202. https://doi.org/10.1016/j.molliq.2019.03.154
17. Mahmoudi C, Chouk R, Baatout K, et al. (2022) Synthesis, characterization and DFT study of new anthracene-based semiconducting polyethers for OLED application. *J Mol Struct* 1251: 131993. https://doi.org/10.1016/j.molstruc.2021.131993
18. Chen B, Inoue S, Ando Y (2009) Raman spectroscopic and thermogravimetric studies of high-crystallinity SWNTs synthesized by FH-arc discharge method. *Diam Relat Mater* 18: 975–978. https://doi.org/10.1016/j.diamond.2009.01.026
19. Pokrop R, Kulszewicz-Bajer I, Wielgus I, et al. (2009) Electrochemical and Raman spectroelectrochemical investigation of single-wall carbon nanotubes-polythiophene hybrid materials. *Synthetic Met* 159: 919–924. https://doi.org/10.1016/j.synthmet.2009.01.056
20. Aarab H, Ba ťoul M, W ćry J, et al. (2005) Electrical and optical properties of PPV and single-walled carbon nanotubes composite films. *Synthetic Met* 155: 63–67. https://doi.org/10.1016/j.synthmet.2005.05.015
21. Wu W, Li J, Liu L, et al. (2002) The photoconductivity of PVK-carbon nanotube blends. *Chem Phys Lett* 364: 196–199. https://doi.org/10.1016/S0009-2614(02)01332-5
22. Baibarac M, Baltog I, Lefrant S, et al. (2007) Spectroscopic evidence for the bulk polymerization of N-vinyl carbazole in the presence of single-walled carbon nanotubes. *Polymer* 48: 5279–5288. https://doi.org/10.1016/j.polymer.2007.07.008
23. Wang C, Guo Z-X, Fu S, et al. (2004) Polymers containing fullerene or carbon nanotube structures. *Prog Polym Sci* 29: 1079–1141. https://doi.org/10.1016/j.progpolymsci.2004.08.001
24. Baibarac M, Baltog I, Lefrant S, et al. (2008) Vibrational and photoluminescence properties of the polystyrene functionalized single-walled carbon nanotubes. *Diam Relat Mater* 17: 1380–1388. https://doi.org/10.1016/j.diamond.2008.01.061
25. Claye A, Rahman S, Fischer JE, et al. (2001) In situ Raman scattering studies of alkali-doped single wall carbon nanotubes. *Chem Phys Lett* 333: 16–22. https://doi.org/10.1016/S0009-2614(00)01335-X
26. Baibarac M, Baltog I, Lefrant S (2009) Raman spectroscopic evidence for interfacial interactions in poly(bithiophene)/single-walled carbon nanotube composites. *Carbon* 47: 1389–1398. https://doi.org/10.1016/j.carbon.2009.01.031
27. Eklund PC, Holden JM, Jishi RA (1995) Vibrational modes of carbon nanotubes; Spectroscopy and theory. *Carbon* 33: 959–972. https://doi.org/10.1016/0008-6223(95)00035-C

28. Henley SJ, Hatton RA, Chen GY, et al. (2007) Enhancement of polymer luminescence by excitation-energy transfer from multi-walled carbon nanotubes. *Small* 3: 1927–1933 https://doi.org/10.1002/smll.200700278
29. Saoudi M, Zaidi B, Alotaibi AA, et al. (2021) Polyaniline: Doping and functionalization with single walled carbon nanotubes for photovoltaic and photocatalytic application. *Polymers* 13: 2595. https://doi.org/10.3390/polym13162595
30. Smida N, Zaidi B, Althobaiti MG (2023) Anthracene/fluorescein based semi-conducting polymer for organic photovoltaics: Synthesis, DFT, optical and electrical properties. *J Mol Struct* 1272: 134088. https://doi.org/10.1016/j.molstruc.2022.134088
31. Mulazzi E, Perego R, W ér y J, et al. (2006) Evidence of temperature dependent charge migration on conjugated segments in poly-p-phenylene vinylene and single-walled carbon nanotubes composite films. *J Chem Phys* 125: 014703. https://doi.org/10.1063/1.2212388
32. Wieland L, Li H, Rust C, et al. (2021) Carbon nanotubes for photovoltaics: From lab to industry. *Adv Energy Mater* 11: 2002880. https://doi.org/10.1002/aenm.202002880
33. Abudulimu A, Eckstein K, Gemayel ME, et al. (2022) Single-walled carbon nanotubes as an additive in organic photovoltaics: Effects on carrier generation and recombination dynamics. *Solar RRL* 6: 2101010. https://doi.org/10.1002/solr.202101010
34. Bertoncello P, Notargiacomo A, Erokhin V, et al. (2006) Functionalization and photoelectrochemical characterization of poly[3-3′(vinylcarbazole)] multi-walled carbon nanotube (PVK-MWNT) Langmuir-Schaefer films. *Nanotechnology* 17: 699–705. https://doi.org/10.1088/0957-4484/17/3/014
35. Wu H-X, Qiu X-Q, Cai R-F, et al. (2007) Poly(N-vinyl carbazole)-grafted multiwalled carbon nanotubes: Synthesis via direct free radical reaction and optical limiting properties. *Appl Surf Sci* 253: 5122–5128. https://doi.org/10.1016/j.apsusc.2006.11.026
36. Baibarac M, Gomez-Romero P, Lira-Cantu M, et al. (2006) Electrosynthesis of the poly(N-vinyl carbazole)/carbon nanotubes composite for applications in the supercapacitors field. *Eur Polym J* 42: 2302–2312. https://doi.org/10.1016/j.eurpolymj.2006.05.019
37. Huang J-E, Li X-H, Xu J-C, et al. (2003) Well-dispersed single-walled carbon nanotube/polyaniline composite films. *Carbon* 41: 2731–2736. https://doi.org/10.1016/S0008-6223(03)00359-2
38. Zaidi B, Bouzayen N, Znaidia S, et al. (2013) Dynamic properties of the excited states of oligo-N-vinylcarbazole functionalized with single walled carbon nanotubes. *J Mol Struct* 1039: 46–50. https://doi.org/10.1016/j.molstruc.2013.01.057
39. Massuyeau F, Faulques E, Athalin H, et al. (2009) Steady state and transient photoluminescence in poly-p-phenylene vinylene films and nanofibers. *J Chem Phys* 130: 124706. https://doi.org/10.1063/1.3097549
40. Zaidi B, Bouzayen N, Znaidia S, et al. (2013) Dynamic properties of the excited states of oligo-N-vinylcarbazole functionalized with single walled carbon nanotubes. *J Mol Struct* 1039: 46–50. https://doi.org/10.1016/j.molstruc.2013.01.057

AIMS Press